Molecular Crystals
Publication details, including instructions for authors and subscription information:
http://www.tandfonline.com/loi/gmcl15

The Photoelectric Properties of Matrix Isolated Phenanthrene Crystallites in Rigid 3-Methylpentane at 77°K

W. C. Meyer [a b] & A. C. Albrecht [b]
[a] The Dow Chemical Co., Midland, Michigan
[b] Department of Chemistry, Cornell University, Ithaca, New York
Version of record first published: 21 Mar 2007.

To cite this article: W. C. Meyer & A. C. Albrecht (1968): The Photoelectric Properties of Matrix Isolated Phenanthrene Crystallites in Rigid 3-Methylpentane at 77°K, Molecular Crystals, 3:4, 423-460

To link to this article: http://dx.doi.org/10.1080/15421406808082890

Molecular Crystals. 1968. Vol. 3, pp. 423–460

Printed in Great Britain

The Photoelectric Properties of Matrix Isolated Phenanthrene Crystallites in Rigid 3-Methylpentane at 77°K†

W. C. MEYER‡ and A. C. ALBRECHT

Department of Chemistry, Cornell University, Ithaca, New York

Received September 11, 1967; *in revised form December* 18, 1967

Abstract—A spectroscopic and photoelectric study is made of matrix isolated crystallites of phenanthrene in rigid 3-methylpentane (3-MP) at 77°K. The crystallites appear to be optically thin and exhibit persistent internal polarization (PIP) following photosensitization in the phenanthrene absorption region. A variety of studies including lux-ampere experiments strongly support the picture of a bi-excitonic primary charge generation. The charges exhibit lengthy storage properties. They may be directly excited in the near infrared or they may also be excited in the phenanthrene absorption region, the latter probably by an exciton collision. In either case typical polarization and polarization release curves are generated. A small steady photocurrent is also seen which corresponds to electrons passing through the 3-MP matrix. Changes in viscosity of the matrix alters the mobility of the carriers associated with the crystallites. Lux-ampere studies of the peak of the polarization curve show good agreement with the predictions of Rose for an exponential trap distribution. A simple electrical analogue model is developed which fits the polarization decay curve with one parameter and predicts correctly the total accumulated charge during the polarization. The model is based on a specific distribution of charge carrier mobilities suggested by a random orientation of anisotropic crystallites in the applied field. It is suggested that this system may serve as a prototype study for photoelectric examination of photosensitive units of small dimensions.

† Presented in part at the International Conference on Photosensitization in Solids, Illinois Institute of Technology, Chicago, Illinois, June, 1964. This work has been supported by Public Health Service research grant GM-10865 from the National Institute of General Medical Sciences. It is taken in part from the Ph.D. thesis of WCM, Cornell University, June, 1965.

‡ Present address: The Dow Chemical Co., Midland, Michigan.

Introduction

Photoconductivity in dilute, rigid, organic solutions at low temperature has been the subject of recent detailed investigations.[1] Typically, the photoconducting solution consists of an appropriate benzene derivative (such as an amino benzene) dissolved in 3-methylpentane (3-MP) and cooled to 77°K. When excitation is in the region of solute absorption, primary photocurrents are observed and, following this, new, secondary, photoelectric signals appear when exciting in the near IR, visible, or near UV spectral regions. In contrast to this, solutions of aromatic hydrocarbons showed no photoelectric activity whatever. However, whenever the concentration of the aromatic hydrocarbon was such that upon cooling to 77°K a turbidity developed, strong photoelectric signals were seen of a type entirely unlike those seen for the photoconducting solutions.[2] One such turbid system, phenanthrene in 3-MP, has been examined in considerable detail both photoelectrically and spectroscopically. These studies form the basis of the present paper. The spectroscopic study, Part A, serves to characterize the phenanthrene crystallites—particularly with regard to their size. The photoelectric study, Part B, consists of a comprehensive examination of the photoelectric behavior both from a phenomenological and a kinetic point of view. It is found that while exciting the crystallite suspension in the phenanthrene absorption region (near UV) in the presence of an applied field, a persistent internal polarization (PIP) develops, evidently due to the creation of charge carriers in each crystallite whose contact with the 3-MP matrix provides a potential barrier to charge flow. For each individual crystallite this appears to be precisely the "barrier polarization" discussed by Kallman and Pope.[3] The charges remain trapped in the crystallite for a long time and subsequent polarization–polarization release cycles can be generated over and over again with excitation in the near IR or UV regions. The polarization signals are examined from the point of view of field dependence, infrared sensitivity, solvent viscosity effects, storage properties, light intensity kinetics, and oxygen and anthracene

quenching. Finally, a simple electrical analogue is examined in attempting to explain the polarization kinetics.

Experimental

Materials

Purified phenanthrene was obtained from the stock of the late J. Sidman. Purity was checked by comparing the low temperature crystal luminescence of the phenanthrene with that of a phenanthrene–anthracene solid solution. The latter luminescence was identical to that observed by Sidman,[4] while the former consisted of the phenanthrene fluorescence[5] with some anthracene fluorescence superimposed in the long wavelength region of the band. The absence of light absorption above 350 mμ—a less sensitive purity test—signifies that only a trace of anthracene is present. However, evidence cited later proves the anthracene is not involved in the photoconductive process and in fact acts at most as a quenching agent.

3-Methylpentane, the solvent used for the rigid glass, was purified by passing it through a column of Alcoa Activated Alumina. A 1 cm path length of solvent had a transmittancy better than 90% down to 240 mμ.

Apparatus

The identical apparatus employed in the photoconductivity work[1] is used here. An AH-6 mercury lamp was used with a Bausch and Lomb 500 mm focal length grating monochromator to provide light for excitation. The monochromator slits were set to pass a 33 Å bandwidth. The light intensity was varied by using a combination of neutral density filters such that the intensity could be reduced in steps by more than an order of magnitude. A Corning 9863 filter was inserted at the monochromator exit slit to remove stray light. IR light was isolated using a super-pressure mercury HB 0–200 bulb with a filter which transmitted 1–3 μ light.

A John Fluke Model 400 power supply used in conjunction with a voltage divider allowed the field intensity be be varied from 8,000–225,000 V/cm for the electrode spacing employed.

Photocurrents were registered on a Keithley 610 electrometer and, depending upon the experiment, the signals were recorded either on a Tektronix 546 storage oscilloscope or a Leeds and Northrup Speedomax H recorder.

The Pyrex sample cell arrangement is described in detail by G. Johnson.[1,2] Briefly, the sandwich-type cell consisted of semi-transparent (50% transmission) chromium electrodes with a 1 or 5 mil (0.005 inches) Mylar spacer inserted between them.

Procedure

The low temperature absorption spectrum of a dispersion of crystallite phenanthrene in 3-methylpentane was measured for two path lengths and a rigid solution spectrum for a 1 cm path length. The suspension was typically prepared by cooling a 2.9×10^{-2} M solution to 77°K in photometer cells of 5 and 10 mil path lengths. For the rigid solution spectrum, a 10^{-3} M solution was used. A Cary 15 spectrophotometer was employed for all spectra.

Emission spectra were measured for a rigid solution of phenanthrene in 3-MP, a crystallite suspension, and a crystallite suspension with anthracene present as a dopant, all at 77°K. An f/4.5 Aminco grating monochromator using a Bausch and Lomb replica grating blazed for 500 mμ with 600 lines/mm was modified for spectrophotometry (P. Johnson). Exposure times of 5–30 sec were required and the spectra were photographed on Eastman Kodak 103a-F film. A mercury line source was used for reference calibration.

Primary charge generation can only be witnessed in a freshly prepared sample. The charges generated during the primary excitation rapidly build up to the point where the secondary photoelectric events mask the signal due to primary charge creation. In

a freshly prepared sample, when one excites in the phenanthrene band (at 318 mμ, for example), a photocurrent is seen which typically rises to a peak value in about 7 sec. The rise is linear over the first 3 sec. To study the rise kinetics of the primary charge generation, it is necessary to confine measurements to times shorter than 3 sec. Thus a full kinetic study (light intensity dependence) had to be accomplished by short pulses (0.1 sec) of light whose total time of irradiation equalled less than 3 sec in one sample. Each pulse yields a photocurrent spike whose height is proportional to the initial slope. The signal is allowed to decay to dark current before irradiating with the next pulse of light at a different level of intensity. The relative lamp intensity for the wavelengths of interest was determined using an esculin solution as an integrating screen.[6] Reproducibility was assessed by returning to an initial condition for reference; a 10% precision was usually observed. After completing such a set of experiments, the magnitude of the depolarization release signal was found to be less than 1% of that seen following complete polarization of the sample. This was assurance that the secondary photoelectric signals had not yet intruded.

The secondary photoelectric signals appear once primary charge production has been accomplished and the first full polarization of the crystallites completed. Now the polarization release or depolarization shows an extremely rapid rise time (perhaps forty times faster than the initial charge carrier producing step) as do all subsequent polarization or depolarization cycles. These signals were studied using the following sequence: (1) application of the field, (2) sample illumination, (3) cessation of illumination, (4) removal of the field, and (5) re-illumination. Before each new cycle was performed, the sample is irradiated with the field removed long enough to ensure that all internal polarization is cancelled. The rise times of the depolarization spikes were analyzed using an oscilloscope. It was found convenient to use a 2.9×10^{-2} M solution (at room temperature) of phenanthrene for all work; this concentration gives a rigid glass with a densely populated dispersion of crystallites.

Results and Discussion

PART A: SPECTROSCOPIC STUDIES OF CRYSTALLITE SUSPENSION

1. *Absorption Spectra*

The solution absorption spectrum of 10^{-3} M phenanthrene in 3-MP at 77°K is given in Fig. 1 for the first electronic band. Figure 2 presents the low temperature absorption spectrum of a crystalline

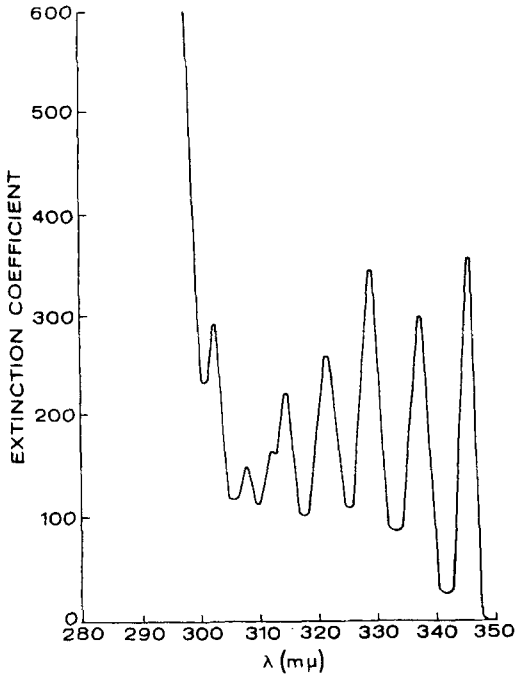

Figure 1. Absorption spectrum of a phenanthrene rigid solution in 3-MP at 77°K.

phenanthrene suspension for 5 and 10 mil path lengths. Several inferences can be drawn by comparing the rigid solution and crystallite spectra with certain results obtained previously by McClure.[5]

The shift in peak positions on going from a rigid solution to the

crystallite dispersion closely matches the pattern observed by McClure[5] for an EPA (ether–isopentane–alcohol) rigid solution of phenanthrene at 77°K and for a single crystal of phenanthrene at 20°K. Table 1 summarizes the results for the most intense peaks.

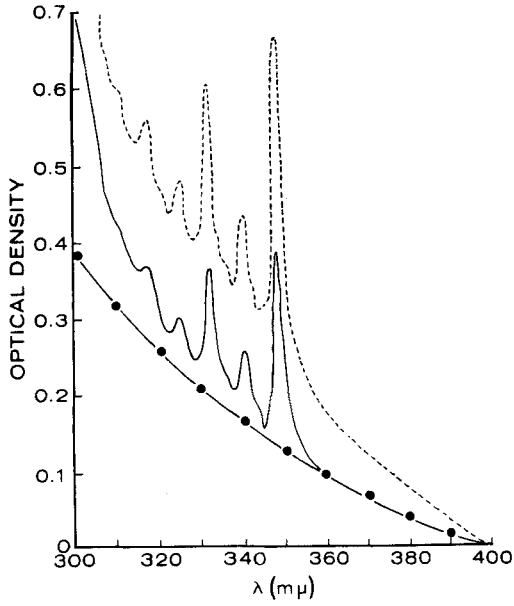

Figure 2. Absorption spectrum of a phenanthrene crystallite suspension in 3-MP at 77°K prepared from a 2.9×10^{-2} M solution. (– – – –) 10 mil path length; (——) 5 mil path length; (●—●) scattered light correction (turbidity).

Evidently the absorption spectrum for the crystallite suspension is derived from actual crystal absorption. (The error in the crystallite column in Table 1 is approximately 100 cm^{-1}.) The fraction of incident light absorbed by the free phenanthrene molecules (about 5% of the sample) dissolved in the saturated rigid glass is negligible.

The well resolved vibrational fine-structure seen in the crystallite spectrum argues for the crystallites being optically thin. In the limit of optically thick crystallites, one would obtain the same featureless spectrum that a single thick crystal with holes would exhibit. The observed fine-structure at optical densities of the

order of 0.60 and less (turbidity corrected) in the 10 mil sample almost certainly means that the individual crystallites themselves possess optical densities of this magnitude or less. If one carries over the phenanthrene molar extinction coefficient from the solution to the crystalline state then the crystals must be considerably thinner than 4 μ to exhibit optical densities of 0.60 or less.

TABLE 1 A Comparison of Absorption Peaks of Phenanthrene in Rigid Solution, in the Single Crystal, and as a Crystallite Suspension in 3-Methylpentane at 77°K

Peak positions			
3-MP rigid glass solution (cm^{-1})	EPA rigid glass solution[a] (cm^{-1})	Crystallite suspension (cm^{-1})	Single crystal (20°K)[a] (cm^{-1})
32 400	32 350	32 210	32 067
31 770	31 780	31 570	31 390
31 010	31 000	30 730	30 688
30 350	30 340	30 030	30 022
29 630	29 590	29 330	29 306
28 930	28 950	28 650	28 660

[a] McClure, D. S., *J. Chem. Phys.* **25**, 481 (1956).

Independently it is possible to assert that the crystallites are less than 7.4 μ thick, since the 5 and 10 mil spectra in Fig. 2 do not follow McClure's[5] results for a crystal of this thickness at 20°K. On the other hand, the qualitative accord between the suspended crystallites and the 1.4 μ thick single crystal absorption spectrum suggests that the crystallites may be even of this thickness or less.

The rapid, smooth rise in background optical density for the crystallite spectrum, in contrast to the absence of this in the solution spectrum, is probably largely due to scattered light or turbidity of the suspension. An estimate of turbidity[7] supports this contention. Although the turbidity contribution at 400 mμ has been arbitrarily set at zero for ease of presentation in Fig. 2, the measured optical turbidity of the crystallites for this wavelength is roughly

0.7 units for a 5 mil thick sample. Thus about 80% of the incident light is scattered at 400 mμ. Light scattering is thus a major phenomenon in the matrix isolated crystallite system. It must also be noted that the photoconductivity experiments were performed with monochromator spectral slit widths equal to or greater than the true half-bandwidth intensities of the vibrational peaks in the phenanthrene absorption spectrum, Fig. 2, so that this low resolution as well as scattered light can influence the wavelength dependence of the photoelectric effects.

When the background turbidity is subtracted from the crystallite spectrum, it is seen that Beer's Law is valid. The absorption data demonstrate that the major portion of the phenanthrene is in the form of crystallites and that these crystallites are optically thin as well. The symmetry behavior of the photoelectric signals with respect to the applied field (see below) also supports the picture of homogeneously illuminated crystallites.

2. *Emission Spectra*

A comparison of the emission spectrum of a rigid solution and that of a crystallite dispersion nicely substantiates the crystallite picture. In fact the presence of a trace of anthracene is found. This is confirmed by comparing the fluorescence of a normal sample to that of an anthracene doped crystallite dispersion. Contribution to the emission from molecularly dissolved phenanthrene is negligible.

Figure 3 presents the luminescence spectrum of a phenanthrene rigid solution at 77°K in 3-MP. Figure 4 illustrates the crystallite fluorescence spectrum under the same conditions. Both solutions are prepared from the same source of phenanthrene. Table 2 compares the results for these two cases with the emission results obtained by McClure[5] for the rigid solution case and a single crystal case. Finally, the luminescence spectrum of an anthracene doped crystallite dispersion in 3-MP at 77°K is given in Fig. 5 and the major peak positions are included in Table 2. This spectrum agrees qualitatively with the results of Sidman[4] for anthracene in dilute

TABLE 2 Fluorescence Peak Positions of Phenanthrene at 77°K Under Different Conditions

3-MP rigid glass solution (cm^{-1})	Methylpentane rigid glass solution[a] (cm^{-1})	Single crystal (20°K)[a] (cm^{-1})	Crystallite suspension (cm^{-1})	Anthracene doped crystallite suspension (cm^{-1})	Anthracene doped crystal (20°K)[b] (cm^{-1})
29 000	28 950	28 240	28 330	—	—
28 600	28 545	27 870	28 000	—	—
28 200	28 095	27 430	27 420	—	—
27 580	27 550	26 900	27 000	—	—
26 800	26 750		26 150	26 150	25 900
26 080	26 160		25 790	25 800	25 600
		25 490	25 480	25 470	25 200
			24 780	24 700	24 600
			23 250	23 200	23 200
				21 830	21 800

[a] McClure, D. S., *J. Chem. Phys.* **25**, 481 (1956).
[b] Sidman, J. W., *J. Chem. Phys.* **25**, 115 (1956), taken from Fig. 4.

solid solution in single crystals of phenanthrene at 20°K. The long wavelength superposition of anthracene fluorescence on the normal phenanthrene fluorescence for a regular crystallite suspension indicates that some anthracene impurity is present for all samples used in this work, but in amounts less than 0.2% since Sidman[4] did

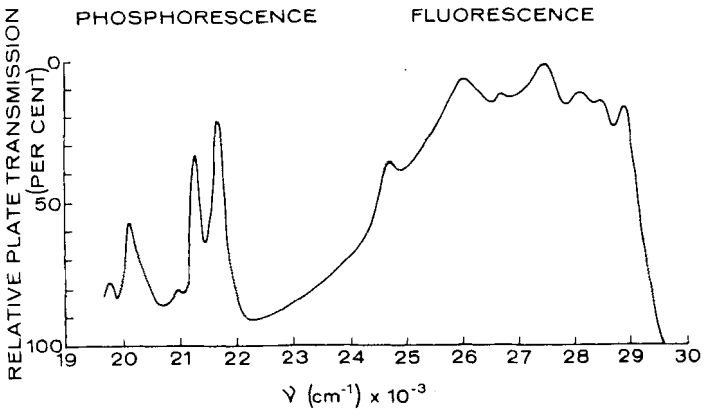

Figure 3. Luminescence spectrum of a phenanthrene rigid solution in 3-MP at 77°K.

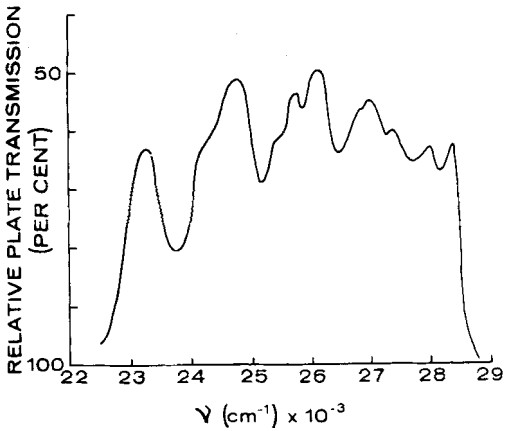

Figure 4. Phenanthrene crystallite fluorescence spectrum in 3-MP rigid glass at 77°K.

not observe any phenanthrene emission for this concentration of anthracene in the phenanthrene crystal.

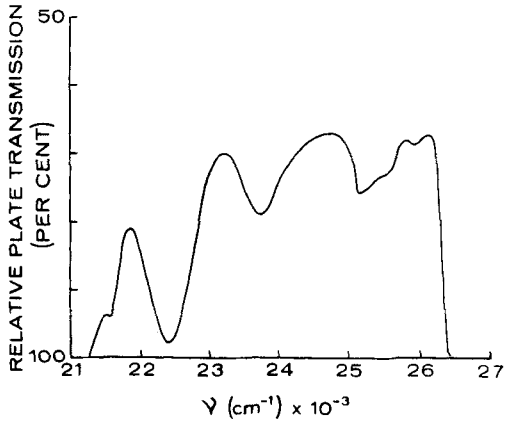

Figure 5. Luminescence spectrum of anthracene doped phenanthrene crystallite dispersion in 3-MP rigid glass at 77°K.

Part B: Photoelectric Studies

A pure 3-MP sample or dilute phenanthrene solution at 77°K shows no photoelectric response in any accessible spectral region. A freshly prepared phenanthrene crystallite suspension shows no photosensitivity in the IR, visible, or near UV region. Only after the phenanthrene crystallite absorption edge is entered is the first photoelectric response seen. This is a slow rise (about 7 sec) to a peak followed by a decay to a weak equilibrium photocurrent. Once this primary sensitization has taken place, the subsequent depolarization or polarization cycles show very rapid rise times and the photosensitivity is extended into the near IR region. In fact, the near IR induced signals and the UV induced signals are almost indistinguishable. A typical polarization signal, followed by an equilibrium photocurrent, and then in the absence of the applied field, the negative depolarization curve are displayed in Fig. 6. This is the signal seen repeatedly once primary sensitization has occurred.

The peak photocurrent, i_p, is typically of the order of 10^{-11} amperes (the illuminated sample area is about 0.3 cm^2), the equilibrium photocurrent, i_e, is less than 10% of this and the total charge polarized is of the order of 10^{-9} coulombs (obtained by integrating over the observed photocurrent less the equilibrium value). These figures vary with conditions, as will be seen below.

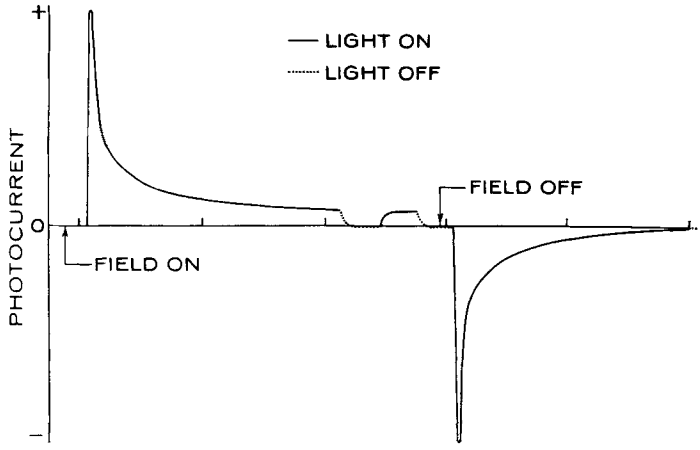

Figure 6. Typical photoeffects of a phenanthrene crystallite suspension in 3-MP at 77°K. Typically, the peak height is of the order of 10^{-11} amperes and the abscissa is marked in units of minutes.

From the outset it is important to establish the major role of the scattered light in generating the photoelectric signals. When a freshly prepared sample is sensitized by irradiating one particular strip of sample, it is found that the photoelectric behavior of a previously unilluminated strip somewhat removed from the sensitized area is actually no different from it. It appears that scattered light, which according to turbidity measurements is more than 80% of the incident light, has successfully acted as sensitizing illumination over large protions of the sample and in general is acting to give photoelectric signals originating outside of the region directly illuminated by the incident beam. Such an effect was never seen when polarization signals were studied using blocking

electrodes in clear rigid glass solutions.[1] Significant light scattering was absent in that study.

We now turn to a variety of studies which, together, serve to characterize the photoelectric behavior of the dispersed crystallite system. Attention is focused on the polarization signal seen (in Fig. 6) only after primary sensitization has taken place. Two portions of this signal are examined. The first is the peak photocurrent, i_p, seen almost immediately after illuminating a sensitized sample in the presence of a field. The second portion of the signal is the equilibrium photocurrent, i_e, seen in the presence of the field but after the polarization of the crystallite has been completed. The total coulombs of charge involved in the full polarization step happens to be proportional to i_p.

1. *Photocurrent–Voltage Relationship*

Figure 7 illustrates the variation of the peak photocurrent and the equilibrium photocurrent with applied voltage. The major portion of i_p must be due to polarization currents set up at the crystallites. It is known[1] that in the presence of UV light the electrode contacts with the rigid solution can serve as ohmic contacts—as the presence of the equilibrium photocurrent demonstrates. On the other hand, blocked electrodes give polarization currents for rigid solutions[1] much like those seen here. The implication is that the crystallite-rigid 3-MP boundary must be essentially a blocking contact to permit the polarization of individual cyrstallites. The symmetry of i_p with respect to the sign of the electrode being illuminated quite likely demonstrates that the crystallites are sufficiently thin to be homogeneously illuminated, or nearly so. We strongly suspect that the major charge carrier in this persistent internal polarization is the electron. In the absence of equal mobility for charge carriers of opposite sign, symmetric behavior of this sort is attributed to a homogeneously produced population of major charge carrier. At the same time the equilibrium photocurrent appears to involve conduction of electrons through the rigid glass. In the rigid solution work[1] identical behavior of the

equilibrium photocurrent was observed as is seen here. A successful fit of the present data was made to the expression.

$$i_e = a(V/L)\,e^{b(V/L)} \tag{1}$$

where V/L is the field strength and values for b found to be $7.7\text{–}9 \times 10^{-7}$ cm-volts^{-1}. The rigid solution work[1] fits the same

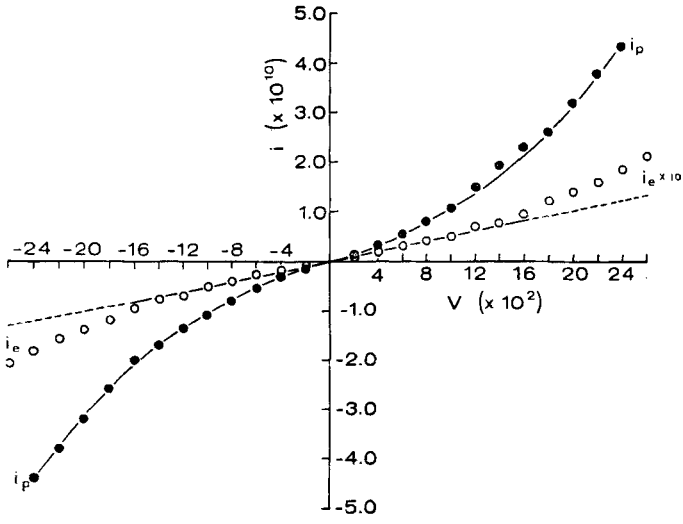

Figure 7. Photocurrent–voltage characteristics for a crystallite phenanthrene suspension with 318 mμ irradiation. (●—●) peak photocurrent; (○—○) equilibrium photocurrent.

expression with b typically near 6.6×10^{-7} cm-volts^{-1}. The behavior of i_p is clearly not the same as i_e (Fig. 7). It has been shown that the value of b depends only on the glass properties, not on the nature of the donor.[1] In the present case the donor must be the phenanthrene crystallite.

The superlinear dependence of i_p on voltage may reflect a field dependence of the charge carrier mobilities within the crystallite or field ionization of trapped charges (the measured applied fields are of the order of 10^5 V/cm). The observed exponent of the voltage

is 1.3–1.6 and is not uncommon.[8,9] Any simple model would predict a linear dependence of i_p on field strength. This is true of the model discussed below as well as that of Many *et al.*,[10] which treats the problem of a partially illuminated photoconducting insulator.

The dependence of i_p and i_e on electrode separation, L, was also studied. At a fixed voltage i_e was found to be linear in $1/L$ as its ohmic behavior at low fields should demand. On the other hand, i_p depended inversely on the 1.4 power of L, in good agreement with the 1.3–1.6 power dependence on V. This means that in this dilute crystallite suspension an average internal macroscopic field is a meaningful concept and the field is effectively uniform across the sample.

2. *Decay Kinetics*

The decay with time of the photocurrent signal from i_p obeys the empirical equation

$$i = A/(t+\theta)^n \tag{2}$$

over a wide range of time (up to 90 sec). A and θ are constants, t the time and n has the value of 0.70 and is independent of the applied field but is a function of the rigid glass used. No particular significance need be attached to the value of θ (~ 0.5 sec) since it is of the order of the instrumental time constant in these measurements.

The decay law and properties of n are identical to the observations of Voglis[11] on wax, glass, and mica dielectric relaxation. A model to be developed below will be strictly for the polarization component of the total signal. Quite a different expression than Eq. (2) will be obtained, and it is moderately successful in fitting the polarization component of the signal with one parameter. It also succeeds fairly well in linking the total charge polarized to $i_p - i_e$, something which Eq. (2) is not capable of doing.

The dark decay of the polarization photocurrent (the collapse of current upon interrupting illumination) was too rapid to be investigated; the decay was exponential with a time constant equal to the instrumental response time.

3. *Infrared Light Stimulation*

The use of 1–3 μ light to study a sensitized sample proved of immense value in acquiring information regarding the behavior of trapped charge. IR irradiation of an electrically polarized sample

TABLE 3 Various Effects of IR Irradiation of the Peak Photocurrent for a 5 Mil Electrode Separation and 2000 Volts Applied

Step	λ	Voltage polarity	i_p (amp)	Comment
(1)	318 mμ	+	1.23×10^{-10}	UV polarization with sample neutral but sensitized.
(2)	IR	0	-6.6×10^{-11}	IR depolarization
(3)	318	+	1.02×10^{-10}	Almost complete UV recovery.
(4)	IR after 3 UV cycles	0	-7.5×10^{-11}	No gradual buildup of IR sensitive trapped charge.
(5)	IR	+	4.6×10^{-11}	Little charge recombination. (IR can polarize sample.)
(6)	IR	0	-3.9×10^{-11}	Primarily only charge redistribution involved.
(7)	IR	+	3.9×10^{-11}	Constant peak value reached by IR cycles.
(8)	318	0	-8.4×10^{-11}	UV depolarization.
(9)	IR	+	6.6×10^{-11}	Little recombination for UV depolarization.
(10)	318	0	-9.0×10^{-11}	UV and IR behavior equivalent.
(11)	318+IR	+	1.86×10^{-10}	IR acts as increase in overall light intensity.
(12)	318+IR	0	-1.92×10^{-10}	Same as (11).
(13)	318	+	1.4×10^{-10}	Sample in almost same state as in (1).

with the field removed gives a depolarization photocurrent comparable to UV depolarization with identical decay characteristics. Complete depolarization of the sample can be achieved with the use of IR stimulation as evidenced by almost total recovery of the UV polarization signal in the next cycle. Various observations of the

sample for IR stimulation are summarized in Table 3 in sequential form. Values of i_p are listed but these are directly proportional to the total coulombs polarized. The absence of any significant increase in the IR depolarization spike after several cycles of UV illumination indicates there is no gradual build-up of charge in shallow traps; rather the preponderance of traps lie in the IR region, a condition not unexpected if the trap distribution is not continuous in energy below the crystallite conduction band. There is evidence that IR depolarization leads to no or little charge recombination, but only a reshuffling of the electrons (and possibly holes) into a new equilibrium condition, since a depolarized (neutral) sample with a field present can now be polarized again using IR light. Several repetitions of the IR cycle cause the peak photocurrent to steadily decrease until a constant value is reached. Whether this is due in part to recombination or leaking of electrons trapped in the crystallite into the surrounding rigid medium or a combination of both is not known.

Evidently depolarization in the UV region does not destroy the ability to polarize again with IR light. The depolarization in the UV is very likely the same process occurring in the IR—the reshuffling of previously generated charges that are shallowly trapped. There seems to be little fresh charge-pair generation playing a major role in any of the UV produced signals. Apparently the trapped electrons and holes comprise a system independent of each other within the crystallite; although there is considerable movement of charge, recombination is relatively minor. This must imply that the density of traps is so large that the probability of trapping overwhelms by far the probability for recombination.

The similarity of the two wavelength regions is further demonstrated by the fact that complete depolarization at one energy leaves no further photosensitivity at the other energy. The same charge carriers are thus involved for both cases and furthermore, they behave independently of the energy used for their detrapping. Additional support comes from simultaneous irradiation with 318 mμ and the IR light. The peak height is increased by 1.5 over that for 318 mμ alone, but the area under the current–time curve (the

total charge released) remains unchanged. The fact that no difference exists between depolarizing with strongly absorbed UV light with an accompanying exponential (or linear for thin crystals) attenuation of light through the crystallite and depolarizing with uniform IR penetration is further evidence that the crystallite must be homogeneously illuminated in the UV region. It would be expected that UV light should be less effective as a detrapping agent if it is entirely absorbed at the front surfaces of the crystallites.

4. *Viscosity Effect*

When isopentane is added to 3-MP, rigid glasses of much lower viscosity are formed when the solution is cooled to 77°K than for

TABLE 4 Viscosity Effect on Photocurrent for 5 Mil Electrode Spacing and 2600 Volts Applied

Rigid glass	Viscosity[a] (P)	λ	i_p (amp)	i_e (amp)
3-MP	9.14×10^{11}	318 mμ	1.68×10^{-10}	1.1×10^{-11}
		IR	1.65×10^{-10}	
80% 3-MP 20% isoP	6.2×10^{10}	318 mμ	8.8×10^{-10}	2.1×10^{-11}
		IR	4.1×10^{-10}	
40% 3-MP 60% isoP	1.8×10^{8}	318 mμ	1.2×10^{-9}	2.2×10^{-11}
		IR	4.2×10^{-10}	

[a] Lombardi, J. R., Raymonda, J. W., and Albrecht, A. C., *J. Chem. Phys.* **40**, 1148 (1964).

3-MP alone.[12] In the softer glass, the phenanthrene crystallite photocurrents rise and decay with much faster times. Table 4 summarizes the change in peak photocurrent in going to less viscous media. The dramatic increase in i_p for the softer glasses is more pronounced for a small viscosity change near the 3-MP viscosity, and becomes less once initial softening has occurred. Saturation of the IR peak and i_e is reached by the time the viscosity has dropped an order of magnitude. The total charge detrapped in

the two softer glasses is the same even though i_p changes substantially.

The increase in i_p for UV and IR excitation in the less viscous media may be explained on the basis of an increase in the mobility of the charge carriers within the crystallites. This could come about, for example, if the crystallization pattern in the softer glasses favored more perfect crystallites. An attempt to anneal the high viscosity 3-MP sample was made to see if the polarization spikes would increase and also sharpen, i.e., to simulate a soft glass effect. After irradiating the sample for 4 min with incandescent light, i_p was increased 1.5 times over that of a regular sample, but dropped to 1.1 times as great for a second polarization cycle. Since it has been observed[13] that strains often reappeared from 5–15 min after annealing, it is probable that in our case the glass temperature was raised to remove strains and the first cycle was carried out before the sample recovered thermal equilibrium. The second cycle was performed in the time interval where strains would reappear. The simulated soft glass effect supports the proposal that the mobility is increased as the viscosity decreases.

The slight increases in i_e on going to softer matrices agree with the steady-state behavior seen in the rigid solution results[1] as does the absence of an IR effect in the softer glasses for both cases. This implies that i_e is associated with glass rather than crystallite conductivity (as we concluded earlier); the absence[1] of IR sensitive traps in the mixed solvent glasses explains why no IR effect is seen.

The decay kinetics of crystallite current in these glasses follow the same rate law as in the 3-MP medium with n equal to 0.96 and θ equal to 2.3 sec. The softer glasses can be considered to be a different dielectric material.

5. *Storage Properties*

The thermal release of trapped charge can be measured by the decrease in the depolarization spike with time of dark storage of a polarized sample. Figure 8 gives the results for the three solvents used. It is interesting to note that storage properties are solvent independent, in contrast to the photoelectric properties.

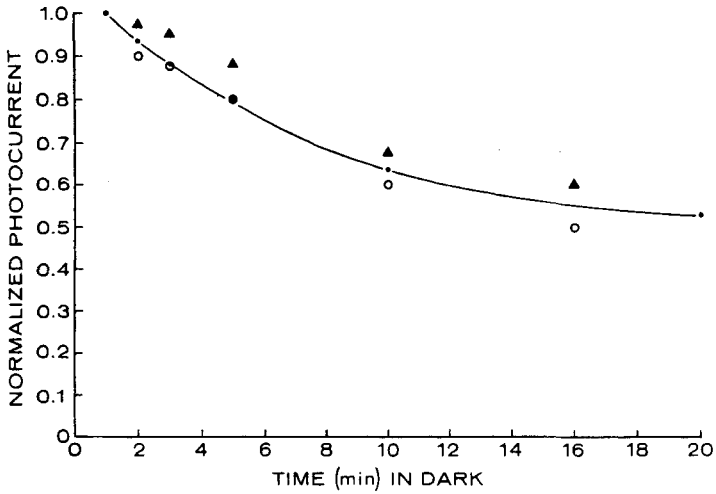

Figure 8. Storage properties of trapped charge in dark for different rigid glasses. (●) 3-MP; (○) 80% 3-MP, 20% isoP; (▲) 40% 3-MP, 60% isoP.

6. *Light Intensity Dependence*

(*a*) *Peak photocurrent as a function of intensity*

The peak photocurrent for polarization or depolarization was found to obey the relation $i_p \propto I^n$ with an average value of n equal to 0.72 for all wavelengths of excitation in the phenanthrene absorption region. The model of Many *et al.*[10] predicts a linear dependence as can ours (see below). A breakdown of these models would occur in the event i_p is influenced by a trap distribution in energy. It happens that the model of Rose[14] for an exponential trap distribution yields an equation where the concentration of conduction electrons has a power dependence on the incident light of $T_1/(T + T_1)$ where T is the temperature at which the experiment is carried out and T_1 is a characteristic temperature of the traps, physically equated to the temperature at which they are frozen in as the sample is cooled. It is interesting, though perhaps coincidental, how the present system fits this model. The experimental exponent of 0.72 and for $T = 77°K$ gives $T_1 = 198°$. This should correspond to the temperature at which the traps are formed. The

temperature at which precipitation of phenanthrene begins should be close to or the same as T_1, since the traps in the crystallites would be expected to form at this time rather than at the glass transition temperature. The 2.0×10^{-2} M sample was found to reach 211°K before onset of precipitation. This is in close agreement with the predicted value. An additional check was made using a dilute 2.3×10^{-3} M sample. Precipitation did not commence until 117°K. The predicted exponent of 0.60 is in excellent accord with the observed value of 0.62. A similar trap distribution was proposed to account for the results of a surface cell of crystalline anthracene.[15]

(*b*) *Initial slope for* i_p *as a function of intensity*

The rapid rise of photocurrent with time leading to i_p in the depolarization (or subsequent polarization) cycle is a measure of the

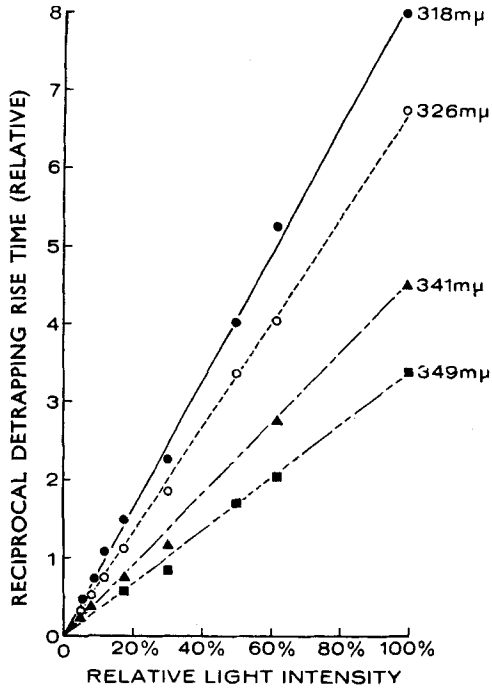

Figure 9. Light intensity dependence of reciprocal detrapping rise times.

rate of photoionization of trapped charge. This is clear from the results of IR stimulation since only trapped charges are photosensitive in this region. Data on initial carrier production given below also bear this out. The linear dependence of the slope on light intensity for all wavelengths (an average experimental exponent

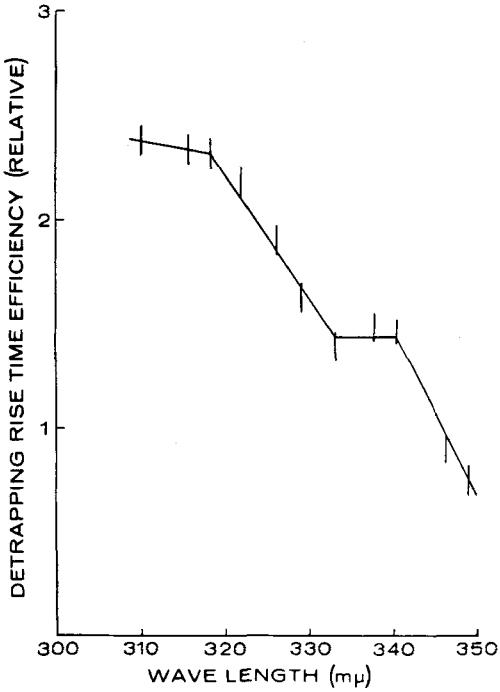

Figure 10. Excitation spectrum of reciprocal detrapping rise times.

of 1.03) is apparent from Fig. 9. The ionization of trapped charge in the crystallites is, therefore, a one photon process, not unlike that observed for detrapping in the rigid glass.[1] The excitation spectrum for this ionization is presented in Fig. 10. The reciprocal rise times have been normalized to constant photons incident and can be considered proportional to a quantum efficiency. The excitation spectrum represents the wavelength dependence of trap ionization.

It is significant that negligible detrapping signals are observed

with illumination of the high intensity mercury lines of the light source in the region 350–600 mμ for a polarized sample. Since phenanthrene does not absorb in the region used for IR depolarization, it follows that this detrapping process is a result of direct ionization of trapped charge with the trapping sites being the primary absorber. For UV detrapping in the phenanthrene absorption band, direct absorption of light by the trapped charge is unlikely—otherwise one would expect a panchromatic response extending beyond the phenanthrene band edge to longer wavelengths. It is concluded that phenanthrene is the primary absorber in this region and acts as a sensitizer for freeing the trapped charge. To account for the high efficiency of the UV detrapping process, the trapping sites must preferentially capture the excitation energy of the phenanthrene (perhaps excitons) and become ionized before the energy thermally degrades. If this is true, the excitation spectrum of the reciprocal detrapping rise time (Fig. 10) for UV excitation should follow the crystallite absorption spectrum. The absence of detailed structure in the action spectrum can be accounted for by considering the large amount of light scattering found to be present. If the turbidity overwhelms the structural details in the true spectrum, the action spectrum for detrapping should follow the wavelength variation in turbidity. It has been shown earlier that reabsorption of this light causes polarization to occur in dark regions adjacent to the illuminated strip and the trend in the detrapping spectrum does conform qualitatively to the prediction.

(c) *Equilibrium photocurrent as a function of intensity*

The variation of the equilibrium photocurrent with light intensity was found to be linear also (0.96 dependence experimentally) for all wavelengths. Figure 11 gives some selected results. It can be shown[7] how a linear light intensity dependence for a steady state signal agrees with kinetic predictions formulated for pure one-photon produced steady state photocurrents if only photoionizable traps are present in the glass and thermally ionizable traps are unimportant. Thus the ejection of charge from the crystallite into the rigid environment proceeds through a one-photon ionization. In

contrast, it can be shown[7] how in order to explain powers of intensity less than unity, such as seen for i_p in the crystallite, traps which are more readily ionized thermally than radiatively must be important. According to these results, then, the crystallite contains a much larger density of shallow traps (thermally ionizable) than

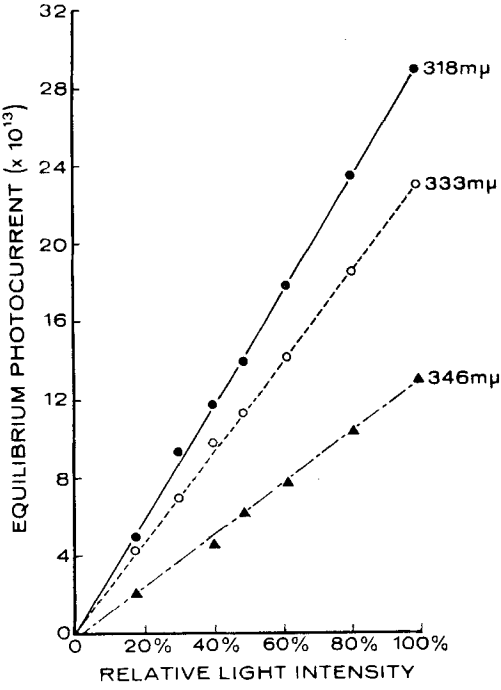

Figure 11. Light intensity dependence of equilibrium photocurrent.

does the rigid glass, and, incidentally, it is electrons in these traps which would be field ionizable.[1] The stronger sensitivity of i_p to field strength than i_e (see Fig. 7) agrees with this picture.

Figure 12 depicts the action spectrum for the dependence of the equilibrium photocurrent on exciting wavelength. The similarity between this spectrum and the crystallite detrapping wavelength dependence (Fig. 10), when viewed with regard to the results of initial carrier generation to be given below, points to a common

origin of the two photocurrents—namely the one-photon ionization of trapped charge at the crystallites. The steady (equilibrium) photocurrent would correspond to a process where the crystallite acts as an electron donor to the rigid glass, with a steady state condition established between electrode—rigid glass—crystallite—rigid glass—electrode movement of charge.

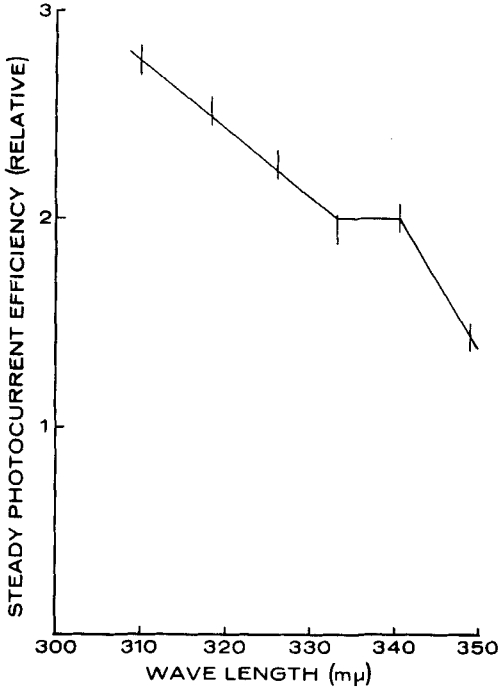

Figure 12. Excitation spectrum of equilibrium photocurrent.

(*d*) *Initial carrier production*

We now turn our attention to the mechanism of initial charge generation for a sample *with no prior illumination.* Figure 13 illustrates the change in initial slope of photocurrent with light intensity for such a sample (determined as outlined in the experimental section). The wavelength study is given in Table 5 for

various types of excitation. The light intensities and initial slopes in Table 5 are relative values.

The strong superlinear approach to a quadratic intensity dependence is perhaps not as clearly defined as desired and might be better researched through transient photocurrent investigations

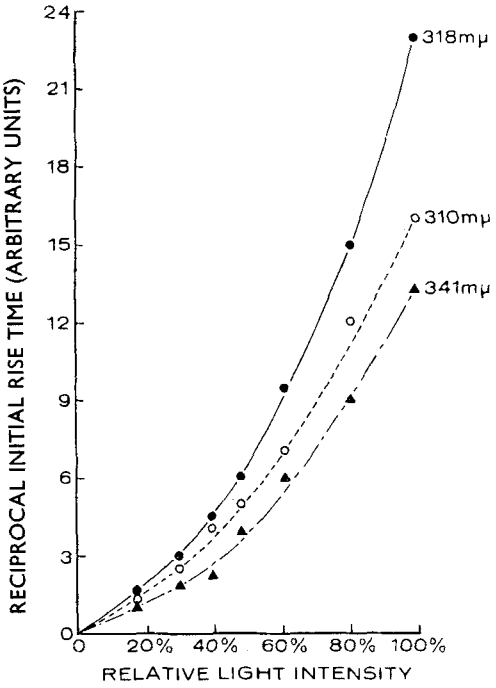

Figure 13. Reciprocal initial rise time variation with light intensity.

using shorter light pulses. Part of the lack of clarity lies in the rapid emergence of light sensitive trapped charge which tends to overwhelm the quadratic character and shift the dependence towards linearity. This condition is already present when the peak current is reached for continuous illumination, where IR irradiation causes a slight photocurrent increase.

One striking difference between the crystallite and rigid solution biphotonic behavior is the insensitivity of the crystallite system to

simultaneous double beam irradiation with one beam in the absorption spectrum of phenanthrene and a second beam outside of this region. This eliminates one possible mechanism of charge carrier generation. In the rigid solution study a two-beam experiment changes the biphotonic character into separate linear dependencies for two beams of comparable intensities, lending support to the picture that a long-lived intermediate state is

TABLE 5 Light Intensity Dependence of Initial Carrier Generation

Excitation mμ	Light exponent	Light intensity (Rel)	Initial slope (Rel)
310	1.76	0.41	0.32
318	1.85	0.85	1.00
326	1.92	0.71	0.55
333	1.85	1.00	0.77
341	1.74	0.72	0.45
349	1.71	0.65	0.23
318+IR (double beam)	1.47		
333+IR ,,	1.87		
318+365 ,,	1.63		
333+365 ,,	1.97		

involved in that photoionization process. Here the coincidence for the energy threshold of the second photon with the threshold of phenanthrene absorption strongly supports a bi-excitonic mechanism of ionization, but does not exclude other mechanisms. Crystal exciton–exciton interaction has been postulated to explain charge carrier production in crystalline anthracene photoconductivity.[16–19] A quadratic light intensity dependence for transient photocurrents is observed for weakly absorbed light and becomes linear for strong absorption.[17] The discrepancy between the observed linear dependence for strong absorption and the predicted quadratic dependence is surmounted by proposing strong surface recombination to bring experiment and theory in line.[18] In our matrix isolated crystallite system the proven absence of any

significant recombination in the phenanthrene crystallite system and the data which support weak absorption of light by the individual crystallite should make this system ideal for observing direct exciton–exciton interaction effects. The circumstances seem to bear this out.

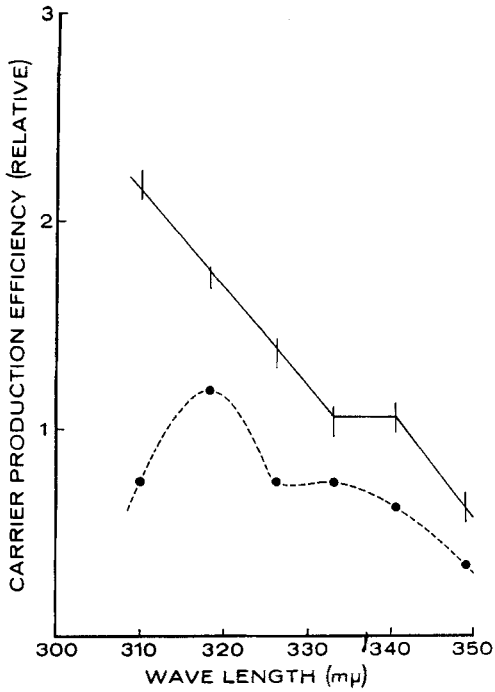

Figure 14. Excitation spectrum for initial carrier production reciprocal rise times. (/—/—/) ordinate normalized with respect to I_0^2; (●---●) ordinate normalized with respect to I_0.

For a bi-excitonic mechanism, the initial slope of charge generation should vary as the square of the incident photon flux and follow the crystallite absorbancy. Figure 14 presents the excitation spectrum for initial carrier production. The ordinate is the initial slope normalized with respect to I_0 and I_0^2. Comparing the excitation spectra of initial rise times to detrapping rise times, close

agreement is appearent for I_0^2 normalization but not for I_0. If the detrapping excitation spectrum is taken as the overall light absorption spectrum of the system, including light scattering contributions, for the experimental conditions used, then the action spectrum for initial carrier generation follows the crystal absorption for current production when a two-photon (exciton) process is presumed. (It is thereby assumed that the quantum efficiency for detrapping is wavelength independent.) The "anomalous" behavior of the one-photon action spectrum for initial carrier generation does not in itself prove that this process is not a one-photon event, but it strengthens the contention that a two-photon process is involved and supports the light intensity dependence results (Table 5).

The UV excitation spectra for reciprocal detrapping rise times, equilibrium photocurrent, and the I_0^2 normalized initial carrier generation all conform qualitatively to the turbidity curve behavior and closely resemble one another. Omitting the possibility of coincidence, it is concluded that in the UV case one single absorption act is common to (1) the detrapping of charge, (2) the generation of a steady photocurrent, and (3) to the initial creation of mobile charge. This act consists of the excitation of phenanthrene with subsequent crystal exciton participation. The important role of scattered light tends to hide the spectral properties of phenanthrene as the primary absorber. A mechanism dependent on scattered light in general, with no specific correlation to phenanthrene absorption, would give photoeffects for excitation beyond the phenanthrene absorption band. The common threshold energy for all photoeffects (around 3500 Å) argues for direct phenanthrene participation in the primary absorption act.

7. *Quenching Experiments*

(*a*) *Anthracene quenching*

A solid solution of anthracene in phenanthrene exhibits only anthracene fluorescence when dissolved in 3-MP and cooled to form

a crystallite suspension in matrix isolation. At the same time the photoelectric signals are quenched to less than 1% of their normal level for less than 1% anthracene contamination of phenanthrene. Thus not only is the primary creation of charge carriers due to phenanthrene, but the quenching of photoconductivity and phenanthrene fluorescence may be derived from the same mechanism. The efficient competition of exciton capture by the impurity against exciton–exciton collision at an exciton trap site to produce mobile charge is reasonable since no photoconductivity is contributed by the anthracene in the phenanthrene system. This absence agrees with the biphotonic nature of anthracene photoconductivity;[16–19] a single exciton capture results only in luminescence, and an impurity exciton–exciton event has negligible probability because of the large separation between anthracene molecules.

The excitation spectrum of anthracene luminescence in the doped suspension resembles very closely the excitation spectra for the three photoelectric signals of phenanthrene. The normalization is with respect to I_0. Since there is general agreement that anthracene receives its energy from phenanthrene by an excitonic mechanism, the excitonic picture for the photoelectric signals is firmly supported.

(*b*) *Oxygen quenching*

A phenanthrene suspension saturated with oxygen displays far less photoactivity than a normal or degassed sample. A room temperature solution was subjected to 20 psi for 5 min and then rapidly cooled. The peak photocurrent for the detrapping process was quenched by a factor of 20. The decrease in the IR signal was identical to the UV decrease. A chemical or photochemical induced oxidation of phenanthrene is excluded for the following reasons. An oxygenated and degassed sample in rigid 3-MP showed no evidence of photochemical decomposition in either sample after illuminating for 45 min at 318 mμ, nor did any new absorption spectra appear from 300–670 mμ. The two samples displayed identical spectra prior to and after irradiation. They showed

identical luminescence spectra, although in the oxygenated sample the luminescence was less intense.

One explanation of the oxygen quenching of photoconductivity is that molecular oxygen is occluded within or adsorbed on the surface of the crystallites and acts as a preferential exciton trap which is highly susceptible to exciton thermal decay. The mechanism of quenching would then be the same as for anthracene quenching, except that the energy is dissipated as heat rather than being partly re-emitted. A second explanation, perhaps equally probable, is one where the oxygen acts as an effective trap of mobile charge, thus inhibiting the buildup of conducting charge. Both processes may be taking place simultaneously.

An Electrical Analogue Model for the Crystallite Suspension

An electrical analogue model will now be sketched for the crystallite suspension. Suppose we say that the kth crystallite, selected at random, projects an area, A_k, onto the electrodes. This area when swept from one electrode to the other in a direction parallel to the applied field defines a unique volume element of the sample for which we shall construct an electrical analogue. It is supposed further that within such an element of volume the chances of finding a second crystallite is negligibly small. One can, therefore, uniquely associate with every crystallite such an element of volume. The material in this element of volume is typically characterized by the sequence: rigid solution (left)—crystallite—rigid solution (right), where the lateral position of the crystallite varies, of course, and may even be at either the extreme left or right. This flexibility in crystallite positioning has no electrical consequence since the properties of an electric circuit having several elements in series do not depend on the sequential ordering of the circuit elements. The lateral positioning of the crystallite simply implies an exchange of places with a portion of the rigid solution.

Formally, each element may act both as a capacitor and a resistor. However, for all practical purposes the rigid glass solution

may be treated as a perfect insulator to give the following simple electrical analogue for the kth element of volume.

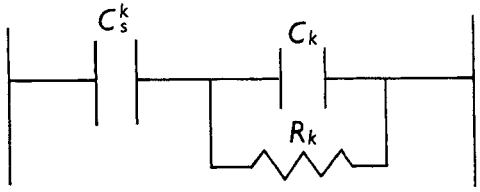

The subscript s refers to the rigid solution element. In general the crystallite is bounded both on the left and right by rigid medium, but as we have pointed out, electrically it is possible to reorder the circuit elements. The above circuit is one of the simple forms.

When a voltage V is applied across this system in the dark essentially nothing happens on an ordinary time scale because R_k is very large. As soon as light is incident R_k decreases by several orders of magnitude so that a detectable current flows on a reasonable time scale. The capacitor C_k will charge until the total voltage drop, V_k, across the crystallite is zero. It will be assumed that neither the capacitance nor the photoresistance of the crystallite changes significantly over this time period. In fact it appears that during a polarization or depolarization phase the number of charges within a crystallite is not seriously altered after the initial photosensitization. This assumption, then, is quite reasonable.

Circuit analysis gives for such a circuit with a constant applied voltage

$$i_k = i_k^0 \mathrm{e}^{-t/\tau_k} \tag{3}$$

where

$$\tau_k = R_k(C_s^k + C_k) \tag{4}$$

and

$$i_k^0 = (V_k^0/R_k)\,(C_s^k/C_k + C_s^k) \tag{5}$$

and the total observed current in the external circuit is just the sum over all such crystallite-containing elements of volume

$$i = \sum_k i_k^0 \mathrm{e}^{-t/\tau_k} \tag{6}$$

If all crystallites have identical properties, τ_k is a constant and the polarization curve should be a simple exponential decay (which it is not). We note that the intensity dependence of i is through that of the factor $1/R_k$ in Eq. (5). Many factors suggest that τ_k must be distributed over a range of values. Distribution in particle size is one obvious factor. However, even granting uniform particle size, there is the interesting question of the random distribution in angular positioning of the crystallites. For anisotropic particles the projected area, A_k will depend on the angular position. It may be, though, that a distribution in A_k does not seriously alter τ_k since in simple geometries resistance is inversely related to cross-section while capacitance is directly proportional to it. On the other hand an anisotropic crystallite can be expected to have anisotropic charge carrier mobility. This could make R_k strongly orientation dependent. The effective R_k is inversely proportional to the effective component of carrier mobility along the direction of the applied field.

The general problem would call for a treatment in which the projection of all principle components of mobility onto the applied field direction is considered both for the positive and the negative charge carriers. The appropriate integrations were not accomplished for the case of arbitrary values of mobility components in a Cartesian framework set in the crystallite. Should the mobility be strongly dominant along some unique direction within the crystallite, then the averaging over all positions is easily carried out. The probability that a given crystallite has its axis of high mobility lying between θ and $\theta + \mathrm{d}\theta$ is just $\sin\theta \mathrm{d}\theta/2$ where θ is the angle between this axis and the direction of the electric field. Recognizing that R_k is inversely proportional to $\cos\theta$ (through the projection of the mobility), one replaces the sum in Eq. (6) by the integral over θ times the total number of crystallites. One now finds

$$i = 2i^0[(1-\mathrm{e}^{-T})/T^2 - \mathrm{e}^{-T}/T] \tag{7}$$

where i^0 is the current at $t=0$ and $T=t/\tau$. τ represents the time constant when the high mobility axis is parallel to the applied field.

Equation (7) with only the one parameter τ offers a better fit than a simple exponential decay. In Fig. 15 a plot is given in which the parameter was arbitrarily fixed at $i = 0.52i^0$ where $t = \tau$. The ohmic component was subtracted from the observed polarization signal.

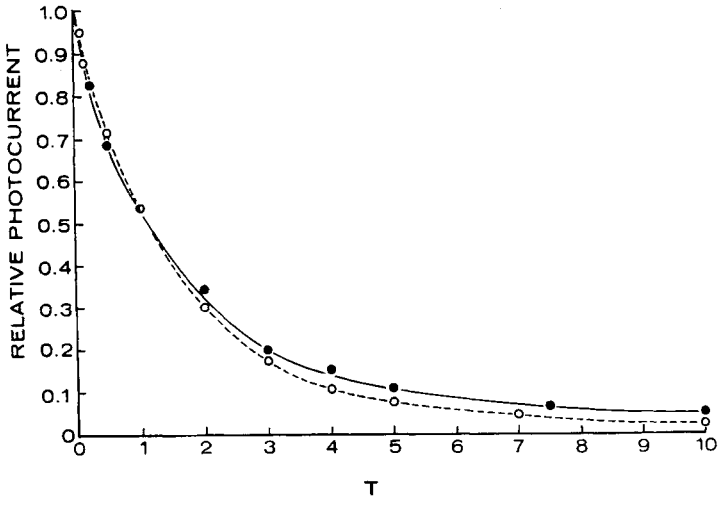

Figure 15. Comparison between photocurrent decay for model and observed decay. (○—○ theoretical; (●—●) observed.

The agreement between the prediction of this model and experiment is fairly striking. It is interesting to note that this functional form, although derived from an angular distribution argument and the assumption of a single major mobility axis, can equally well be derived from an unweighted distribution of crystallite conductivity between zero and the maximum conductivity. A possible physical basis of such a distribution, other than through an orientational effect, is not immediately apparent.

Equation (7) may be integrated over all time to obtain the total coulombs of polarized charge. One finds that

$$Q = 2i^0\tau \tag{8}$$

The i^0 of this equation should correspond quite closely to the $(i_p - i_e)$ of the observed signal. For the data used to fit Eq. (7) it is found that $Q = 5.0 \times 10^{-10}$ coulombs. The predicted value based on Eq. (8) with $\tau = 7.5$ sec from the fit is $Q = 7.4 \times 10^{-10}$ coulombs, in fair agreement with the observed value.

Another test of this model through Eq. (8) is afforded when one notes that the ratio i^0/Q should be field independent as long as τ is field independent. In one sample of 5 mil thickness the voltage was increased from 100 to 2800 volts and $(i_p - i_e)/Q$ varied from about 0.07 to 0.10 sec^{-1}. In another sample of 1 mil thickness, when the voltage was increased over the same range the current to charge ratio increased from 0.08 to 0.14 sec^{-1}. The near constancy of this ratio is thus predicted by this model (as doubtlessly would a variety of models). The general increase of this ratio with applied field could be interpreted as a field dependence of τ through a field dependence of the mobility.

The qualitative success of this model encourages one to concentrate on testing it further with the hope of extracting some physically meaningful parameters.

Conclusions

In summary then, the results of these studies have led to the conclusions that the crystallites are optically thin, that primary charges are generated within them by a bi-excitonic mechanism. The bi-excitonic mechanism is suggested by the strongly superlinear light dependence of primary charge generation, by the very strong quenching effect of charge generation caused by adding anthracene as an exciton trap, and by the coincidence of the energy threshold for both photons with the primary absorption region of phenanthrene. The charges produced have very long storage properties. The polarization and depolarization cycles (Fig. 6) can be generated repeatedly using either near IR light alone, using near UV light alone (in the phenanthrene absorption region), or any combination of the two regions. Visible light does not produce photoelectric signals. Accompanying the polarization current is an

equilibrium photocurrent which exhibits all characteristics of electron transport through the rigid glass system. The trapped charges in the crystallite may be directly released with IR light or indirectly released with UV light via a collision with a phenanthrene exciton. The mobility of the charge carriers in the crystallite can be influenced by the nature (viscosity) of the rigid glass. If the carrier mobility is governed by bulk crystallite properties, then we are forced to conclude that the constitution of the surrounding rigid matrix influences the interior structure of the crystallite. This point brings out a basic question which must be raised. While there is no question but that the PIP is to be associated with the crystallite, by implication we have assumed that all of the crystallite signals are due to charge carrier migration in the *interior* of the crystallite; that is, we are seeing bulk properties. The initial generation of charge carriers is very likely a bulk phenomenon, since both experiments with optically thin crystals and the anthracene quenching point in this direction, however it may well be that the principal region of charge trapping is at the interface of the crystallite-rigid glass boundary and that all subsequent signals in the polarization or depolarization curves result from charge motion on the surface of the crystallites. None of the results presented here would seem to exclude this possibility.

These studies perhaps have made some progress in characterizing photoelectric properties of very small phenanthrene crystallites. However, it is hoped that the principal value of such work may turn out to be its usefulness as a model for the study of a variety of systems dispersed in a rigid organic media. Interesting examples might range from dispersions of possibly photoconducting liquids or polymers to suspensions of various photochemical units to be found in biology.

REFERENCES

1. Johnson, G. E. and Albrecht, A. C., *J. Chem. Phys.* **44**, 3162 (1966).
2. Johnson, G. E., Ph.D. thesis, Cornell University, January 1965.
3. Kallmann, H. and Pope, M., "Charge-Transport Processes in Organic Materials", in Kallmann, H. and Silver, M. (eds.) *Symposium on Electrical Conductivity in Organic Solids* (Interscience Publishers, Inc., New York, 1961), p. 1.

4. Sidman, J. W., *J. Chem. Phys.* **25**, 115 (1956).
5. McClure, D. S., *J. Chem. Phys.* **25**, 481 (1956).
6. Bowen, E. J., *Proc. Roy. Soc.* **154A**, 349 (1936).
7. Meyer, W. C., Ph.D. thesis, Cornell University, June 1965.
8. Raman, R., Azarraga, L., and McGlynn, S. P., *J. Chem. Phys.* **41**, 2516 (1964).
9. Branwood, A. and Tredgold, R. H., *Proc. Phys. Soc.* **76**, 93 (1960).
10. Ben Sira, M., Pratt, B., Harnik, E., and Many, A., *Phys. Rev.* **115**, 554 (1959).
11. Voglis, G. M., *Zeits. f. Physik.* **109**, 52 (1938).
12. Lombardi, J. R., Raymonda, J. W., and Albrecht, A. C., *J. Chem. Phys.* **40**, 1148 (1964).
13. Williams, R., *J. Chem. Phys.* **30**, 233 (1959).
14. Rose, A., *RCA Review* **12**, 362 (1951).
15. Chynoweth, A. and Schneider, W., *J. Chem. Phys.* **22**, 1021 (1954).
16. Northrop, D. C. and Simpson, O., *Proc. Roy. Soc.* **244A**, 377 (1958).
17. Swicord, M., Olneso, D., and Silver, M., *Phys. Rev. Letters* **10**, 12 (1963).
18. Choi, Sand-Il and Merrifield, R. E., *J. Chem. Phys.* **38**, 366 (1963).
19. Kepler, R. G. and Merrifield, R. E., *J. Chem. Phys.* **40**, 1173 (1964).